EvoDevo

RESEARCH

Open Access

Microinjection, gene knockdown, and CRISPR-mediated gene knock-in in the hard coral, *Astrangia poculata*

Jacob F. Warner[1*], Ryan Besemer[1], Alicia Schickle[2], Erin Borbee[3], Isabella V. Changsut[3], Koty Sharp[2] and Leslie S. Babonis[4*]

Abstract

Cnidarians have become valuable models for understanding many aspects of developmental biology including the evolution of body plan diversity, novel cell type specification, and regeneration. Most of our understanding of gene function during early development in cnidarians comes from a small number of experimental systems including *Hydra* and the sea anemone, *Nematostella vectensis*. Few molecular tools have been developed for use in hard corals, limiting our understanding of this diverse and ecologically important clade. Here, we report the development of a suite of tools for manipulating and analyzing gene expression during early development in the northern star coral, *Astrangia poculata*. We present methods for gene knockdown using short hairpin RNAs, gene overexpression using exogenous mRNAs, and endogenous gene tagging using CRISPR-mediated gene knock-in. Combined with the fact that spawning can be induced in the laboratory, during the reproductive window, these tools make *A. poculata* a tractable experimental system for investigative studies of coral development. Further application of these tools will enable functional analyses of embryonic patterning and morphogenesis across Anthozoa and open new frontiers in coral biology research.

Keywords Functional genomics, Spawning, In vitro fertilization, Transgenesis, Scleractinia, Homology-directed repair, Cnidaria, FGF, Minicollagen, TCF

Background

Recent advances in the techniques available for genetic manipulation have opened up new opportunities to perturb and analyze gene function in a broad range of animal phyla [10, 40, 42, 59]. These advancements make it possible to interrogate the evolution of development in taxa representing extreme variation in animal body plans. Among cnidarians, representatives of both Anthozoa (corals, sea anemones, etc.) and Medusozoa (hydroids, jellyfish, etc.) have emerged as highly tractable experimental systems; however, our understanding of development in these clades arises from investigation of only few species. As an example, the molecular regulation of embryogenesis appears to be well-studied in Anthozoa, yet most of our conclusions about this large and diverse

*Correspondence:
Jacob F. Warner
warnerj@uncw.edu
Leslie S. Babonis
lsb257@cornell.edu
[1] Department of Biology and Marine Biology, UNC Wilmington, Wilmington, NC 28409, USA
[2] Feinstein School of Social and Natural Sciences, Roger Williams University, Bristol, RI 02871, USA
[3] Department of Biology, Texas State University, San Marcos, TX 78666, USA
[4] Department of Ecology and Evolutionary Biology, Cornell University, Ithaca, NY 14853, USA

clade of cnidarians derive from studies of the starlet sea anemone, *Nematostella vectensis* [32]. Investigative studies of gene function in other anthozoans have been challenged by lack of accessibility to gametes, protected status of the adult, and a dearth of molecular tools.

The northern star coral, *Astrangia poculata,* is an attractive experimental organism for research on hard coral (scleractinian) development. This facultatively symbiotic, gonochoristic coral is found in high abundance in coastal waterways from the southern Caribbean to Cape Cod MA, USA [12] and is listed by the IUCN as a species of "least concern". In the late summer, when gametogenesis is at its peak in *A. poculata,* colonies can be collected from near-shore locations, induced to spawn ex situ, and their hardy, transparent larvae can be conveniently reared in laboratory conditions [58]. The considerable ease of access to coral colonies combined with the ability to precisely control the timing of fertilization in the laboratory provides the opportunity to genetically manipulate early-stage embryos. Here, we describe the development of molecular tools for investigating gene function during early development in *A. poculata*. These tools establish *A. poculata* as a tractable research organism for functional studies in corals and, more broadly, as a viable system for comparative studies of cnidarian evolution and development.

Methods

Animal collection and maintenance

Fresh colonies of *A. poculata* were collected by divers from Ft. Wetherill, RI, USA and transferred to Roger Williams University. Spawning was induced by acute heat shock (27–28 °C for 1 h) in benchtop containers. After spawning, adult colonies were maintained in a flow-through system with natural seawater and a 12:12 light cycle at Roger Williams University, Bristol, RI.

Microinjection

Astrangia poculata gametes were collected and fertilized in 0.2 µm-filtered sea water and then transferred in filtered seawater to a 35-mm petri dish containing 100-µm mesh (Sefar Nitex 03-100/32) secured to the bottom using modeling clay. Individual zygotes were injected using a fluorescence Zeiss Discovery V8 dissecting scope, Narishige micromanipulator, and Eppendorf FemtoJet 4i picospritzing device, following a protocol developed previously for *N. vectensis* [31]. Two different dextran dyes (Alexa 555 and Alexa 488—Invitrogen D34679, D22910) each diluted to a final concentration of 0.2 mg/ml in nuclease-free water (Ambion AM9937) were used to mark individual blastomeres by injection at the two-cell stage. To assess the feasibility of expressing heterologous mRNA in *A. poculata*, zygotes (one-cell stage) were injected with mRNA encoding an NvTCF-venus fusion protein construct [49] diluted to 300 ng/ul with 0.2 mg/ml RNAse-free dextran in nuclease-free water. Injected embryos were reared at room temperature (~22 °C) for both experiments, mounted in filtered sea water on glass slides, and imaged live on a Nikon Eclipse E800 fluorescent microscope at Roger Williams University.

Transcriptome assembly

Larvae were collected at 12 h post fertilization (hpf), 24 hpf, 36 hpf, 60 hpf, and 84 hpf in Tri-reagent (Sigma T9424) and stored at −80 °C prior to RNA extraction. Total RNA was purified following a protocol previously described for *N. vectensis* [31]. Briefly, samples were processed through two phenol/chloroform extractions and precipitated in isopropanol before being treated for DNA contamination with Turbo-DNAse (Ambion AM1907) for 10 in at 37 °C. Library preparation and 150 bp PE Illumina sequencing (NovaSeq 6000) was carried out by Novogene. Sequencing reads were combined and error corrected using Rcorrector [56]. Adapter trimming and quality trimming were carried out using Cutadapt v3.7 [35] and Trimmomatic v.039 [4], respectively. Cleaned reads were filtered for ribosomal sequences by aligning them ribosomal sequences for *A. poculata* from the SILVA database [44] using Bowtie2 v2.3.4.1 [29]. Unaligned reads were input into Trinity v2.12.0 [20] for assembly and final, assembled transcripts were filtered for sequences longer than 200 bp. Raw sequencing reads and assembled transcripts have been deposited to NCBI under bioproject: PRJNA956119.

shRNA design and synthesis

The *A. poculata* ortholog of FgfA1 was identified using TBLASTN with the *N. vectensis* FGFA1 peptide sequence (NCBI accession: ABN70831.1) [37] as query and the *A. poculata* assembled transcripts as reference. shRNAs were designed and synthesized as described previously for *N. vectensis* [23]. In brief, primers were designed to target the 3′ end of the FgfA1 coding sequence using the Invivogen siRNA Wizard (www.invivogen.com/sirnawizard/design.php) and annealed for 2 min at 98 °C in a thermocycler to generate a template for in vitro transcription. Transcription was performed using the Lucigen Ampliscribe T7 Flash kit (ASF3257) for 5 h at 37 °C in a thermocycler, following the manufacturer's instructions. Products were column-purified using the Zymo Direct-zol RNA Miniprep Kit (R2050), aliquoted, and frozen at −80 °C until the day of microinjection. A scrambled control shRNA was synthesized at the same time using primers described previously [25]. All shRNAs were injected into zygotes at a concentration of 800 ng/µl with 0.2 mg/ml RNAse-free dextran in nuclease-free water. Embryos

were reared to 48 hpf at room temperature, mounted in filtered seawater on glass slides, and imaged live on a Nikon Eclipse E800 at Roger Williams University. Primer sequences for FgfA1 shRNA synthesis are:

Apoc_FgfA1_shRNA_F: TAATACGACTCACTATAGACAACAGCCGCATGACATTTCAAGAGAATGTCATGCGGCTGTTGTCTT

Apoc_FgfA1_shRNA_R: AAGACAACAGCCGCATGACATTCTCTTGAAATGTCATGCGGCTGTTGTCTATAGTGAGTCGTATTA

Fgf inhibitor treatment

Beginning immediately after fertilization, zygotes were incubated in 0.1% DMSO in filtered seawater containing 20 mM SU5402 (Sigma SML0443) for a final concentration of 20 µm SU5402 or 0.1% DMSO in filtered sea water (control). Embryos were reared at room temperature and solutions were refreshed every 24 h until embryos were collected and fixed for immunostaining (48 hpf).

Immunostaining

Astrangia poculata larvae were fixed in 4% paraformaldehyde (PFA) in filtered seawater and washed four times in phosphate buffered saline with 0.1% Tween-20 (PTw) for 5 min each. Non-specific protein interactions were blocked in 10% normal goat serum (NGS) diluted in PTw for 1 h at room temperature. The blocking solution was replaced with a solution containing 1:200 anti-acetylated tubulin antibody (Sigma T6743) diluted in 10% NGS and the samples were incubated overnight at 4 °C. Larvae were washed four times using PTw and incubated in a secondary antibody (Invitrogen A11004) diluted 1:200 in 10% NGS for 2 h at room temperature. Larvae were again washed four times using PTw and counterstained in DAPI (Sigma D9542) diluted 1:2500 and Phalloidin (Invitrogen A12379) diluted 1:200 in PBS overnight at 4 °C. Larvae were washed four times in PTw, mounted in 75% glycerol in PBS on glass slides, and imaged on a Leica Sp8 confocal microscope at UNC Wilmington.

In situ hybridization

Embryos from various developmental stages were collected and fixed for in situ hybridization (ISH) using a two-part fixative series. First, embryos were fixed for 1 min at room temperature in 4% PFA in PTw containing 0.25% glutaraldehyde. This initial fixative was removed and replaced with 4% PFA in PTw and embryos were fixed for an additional 1 h at 4 °C. Excess fixative was removed with three 10-min washes in PTw and tissues were then rinsed once in sterile water to remove excess PTw and twice in 100% methanol before being stored in clean 100% methanol at −20 °C until analysis. ISH was performing following a method developed previously for *N. vectensis* [62], with minor modification. Due the small size and transparency of *A. poculata* embryos, all pipetting steps in the ISH procedure were performed in a sterile 24-well microplate on a dissecting microscope. An antisense mRNA probe directed against the *A. poculata Mcol3* transcript was synthesized as described for *N. vectensis* [62] using the following primers:

Apoc_Mcol3_F:
ATGGCGTCTAAACTCATTCTTG

Apoc_Mcol3_R:
TCACGCGTGCACACACCTA

Tissues were hybridized overnight with the Mcol3 probe diluted to 1 ng/ul in hybridization buffer [62] and signal was visualized using an NBT/BCIP reaction performed in the dark at room temperature. Labeled embryos were washed extensively in PTw to remove excess NBT/BCIP, mounted in 80% glycerol (in PBS) on glass slides, and imaged on a Nikon Eclipse E800 at Cornell University.

CRISPR-mediated knock-in

The *A. poculata* ortholog of *Mcol3* was identified using TBLASTN with the *N. vectensis* MCOL3 peptide sequence (NCBI accession: XP_032218917.1; Uniprot accession: G7H7X1) as query and the *A. poculata* assembled transcripts as reference. The open reading frame was predicted using the NCBI Open Reading Frame Finder (https://www.ncbi.nlm.nih.gov/orffinder/) and sgRNAs targeting the C-terminus of the predicted peptide were designed using ChopChop v3 [28]. Two overlapping guides were designed with the recognition sites CGTGGTCGCTTACTTTCTGC and AATGTCGACGCATCATCACG that cut 4 bp upstream and 11 bp downstream from the insertion site, respectively. Single guide RNAs (sgRNAs) were synthesized by Synthego (Redwood City, CA, USA) with the default 2′-*O*-methyl modification at the 3 first bases and 3′ phosphorothioate bonds between the first three and last two bases.

Knock-in repair templates were synthesized using PCR. To do this, primers were designed to contain 40-bp homology arms that are homologous to the insertion site (immediately 5′ and 3′ to the predicted stop codon), a two-alanine spacer, and 15 bp to bind and amplify mNeonGreen in frame with the open reading frame. Silent mutations were introduced in the sgRNA recognition sequences to prevent recutting from sgRNAs. The oligo sequences were as follows (*Apoc* homology sequences, sgRNA mutations, [linker], **mNeon priming region**):

Apoc_Mcol3_Homology_F:
5′GCGTCTCGTCCTGCCCGACCCAGTGCTGCTCCGGGAGGAAA[GCCGCA]**ATGGTGAGCAAGGGC**3′

Apoc_Mcol3_Homology_R:
5′TAATTTCTAAATCTCGTGCTAATGTCGACG CATCAAGTGCTCGTGGC**TTACTTGTACAGCTC GTC**3′

PCR amplification of the repair template was performed using 50 ng of plasmid containing mNeonGreen (Addgene 125134) as template in a touchdown PCR reaction (annealing temperature decreased 1 °C from 65 °C to 50 °C for the first 15 cycles followed by 20 cycles with an annealing temperature of 50 °C; extension time was 30 s). Afterwards, the template was digested by addition of DpnI enzyme (NEB R0176S) and incubation at 37 °C for 2 h. The repair template was then purified using a QiaQuick PCR purification kit (Qiagen 28704 prior to injection and quality assessed using agarose gel electrophoresis, to ensure size, and Nanodrop, to assess purity and concentration.

The injection mix was assembled as follows:

150 ng/µl final concentration of dsDNA repair template
200 ng/µl final concentration of ApMcol3 sgRNA1
200 ng/µl final concentration of ApMcol3 sgRNA2
0.5 µl of Cas9 protein (IDT 1081060)
Alexa-555 dextran (0.2 mg/ml)
Nuclease free water to 5 µl.

Ribonucleoprotein (RNP) assembly was promoted by incubation of the injection mix at room temperature for 15 min prior to injection. Genome edited individuals were generated by performing two rounds of injection on different days.

Imaging and genotyping knock-in mutants

Mutant embryos were identified using a fluorescent dissecting scope, mounted on glass slides in filtered sea water, and imaged live on a Nikon Eclipse E800 fluorescent microscope at Roger Williams University. Selected mutant knock-in larvae (48 hpf) were transferred individually to 0.5-ml PCR tubes and gDNA was extracted from individual larvae as previously described [54]. Wild type gDNA was extracted from uninjected 48hpf larvae from the same spawn. PCR was used to amplify the knock-in locus and insert size was confirmed using gel electrophoresis. Genotyping primers are as follows:

Apoc_Mcol3NG_F:
GGACCATCTGGACGAATGGGAC
Apoc_Mcol3NG_R:
CAATTCGCTCTTCTCTGCCTTCTAT

Predicted gene sequences

Astrangia poculata Minicollagen 3 (constructed from multiple overlapping assembled transcripts, *=stop codon location):

ATGAAAGACTCAACGACTGTCGAAATACAG
CCTTATTCAAGCACATTTCAAAGATCGCTAGCC
TGGGATCCAGAGATGGCGTCTAAACTCATTCTT
GGGTGCTTAGCACTCATGGTAGTGTCGACCTAC
GCCAGATCAACATACAAAAGAAGCGCTAACCCG
TGTCCCCCGGGATGTCCCGGTAGTTGTGCGCCC
TCGTGTGCGGTGTCTTGTTGTCTTCCTCCACCA
CCCGCTCCACCACCGCCCCCACCCCCACCCCCA
CCACCACCAGAGCCCGCTAAGCCCGGACCACCT
GGACCATCTGGACGAATGGGACCACCCGGACCT
GTCGGACCTATCGGACCCATGGGAGAGGCCGGA
CCACCTGGAATACCCGGACCCCAAGGACCTCCT
GGACCTCCCGGAGAACCCGCTCCTCCACCACCA
CCACCCCCACCGTGCCCACCTGTCTGCGCCCAC
ACATGCGTCTCGTCCTGCCCGACCCAGTGCTGC
TCCGGCAGAAAGTAA*GCGACCACGTGATGA
TGCGTCGACATTAGCACGAGATTTAGAAATTAC
TCCAACTTTAGCGTTCGTAAAGTACTTTTTCAG
TGGA

Astrangia poculata FGF1A (CDS extracted from transcript TRINITY_DN12668_c0_g1_i4):

ATGAATTCCATTCAACTGCTTTTCCTACTTCAA
CTCTTTTGCTTCACGGAGATAAACACTTCAGCT
AAACCGTACAACGCAACCAAATCCCAGACTAAA
GATGCCGCGAGAACTTCAAGAGGATCTATCTCA
TCATCCATGACCAGATACGAAAACGACAGAATC
AGAAACCATTCCCGAAAAACATTTCTTTCCAAG
AAGCAGAAATGGCCACAACCGTCCACGGAAAGT
TCCTTGAAACGTGTCCGCAAAATAACAAAACGA
CCGACAGCTACAACGCACTGTAAAATATTCTGC
CGCAGCGGTTATCATCTTCAAATCCTTCCCAGT
GGTGCAGTGAGGGGGACGGTTGACCAGGGC
AGCAAGTACGTGTTGTTTGAGATGCAGTCATTT
GGCCCTAGTCTCGTCAGGCTGATGAGTACAGCG
ACGGGCAGGTACCTATCTATGAGAAGAGACGGG
AGTCTTCGAGGGTTGCGTAGCCAAAGTAACCGG
GACTCACTTTTCAAAGAGACACATGAACAGAAC
GCGTTTCACTCTTACGCGTCACACAGATATTAC
AGACAACAGCCGCATGACATGTTGGTTGGCATC
AAGAGAAACGGACAAATAAAACGAGCCACTAAA
ACCTTGCATGGACAAACTGCTACGCAATTTCTT
GTCATCAAATTTTAA

Quantification and statistical analysis

Quantitative analysis of apical tuft morphology was performed by measuring the maximum length of the longest aboral cilium and the length of the body axis (mouth to apical tuft base) in individual embryos using the Measure

Tool in Fiji V1.54b [52]. All data were analyzed in the R statistical computing environment V4.2.1 [47].

Results and discussion

Spawning and microinjection of *Astrangia poculata*

To establish methods for manipulating gene function during embryogenesis in *A. poculata,* we collected wild adult colonies and induced spawning at precise times by raising the water temperature quickly from 19.5 °C to 27–28 °C in benchtop containers. Gamete release began 1–1.5 h after heating (Fig. 1A, B). To perform microinjection, we concentrated fertilized zygotes in a small volume of seawater and pipetted them gently onto the top of a piece of 100-µm nylon mesh secured with modeling clay to the bottom of a 35-mm petri dish filled with filtered sea water (Fig. 1C, D). The nylon mesh serves to cradle the individual zygotes during microinjection and the clay ensures the mesh can be removed easily to facilitate recovery of injected zygotes. At room temperature (~22 °C), first cleavage occurs after approximately 90 min, allowing for injection of a large number of zygotes. First cleavage in *A. poculata* is holoblastic, resulting in complete segregation of the first two embryonic cells. We demonstrated this by injecting two different dyes at the 2-cell stage and observing conserved segregation of the dyes later in development (Fig. 1E). By contrast, in *N. vectensis* complete segregation of embryonic cells is not observed until the 8-cell stage [17]. Thus, single-cell injections at the 2-cell stage in *A. poculata* could be used to knockdown or overexpress gene products in half of the embryo, facilitating studies of cell–cell communication during early development. To test the feasibility of using exogenous mRNAs for over- and mis-expression assays in *A. poculata*, we injected mRNA encoding a transcription

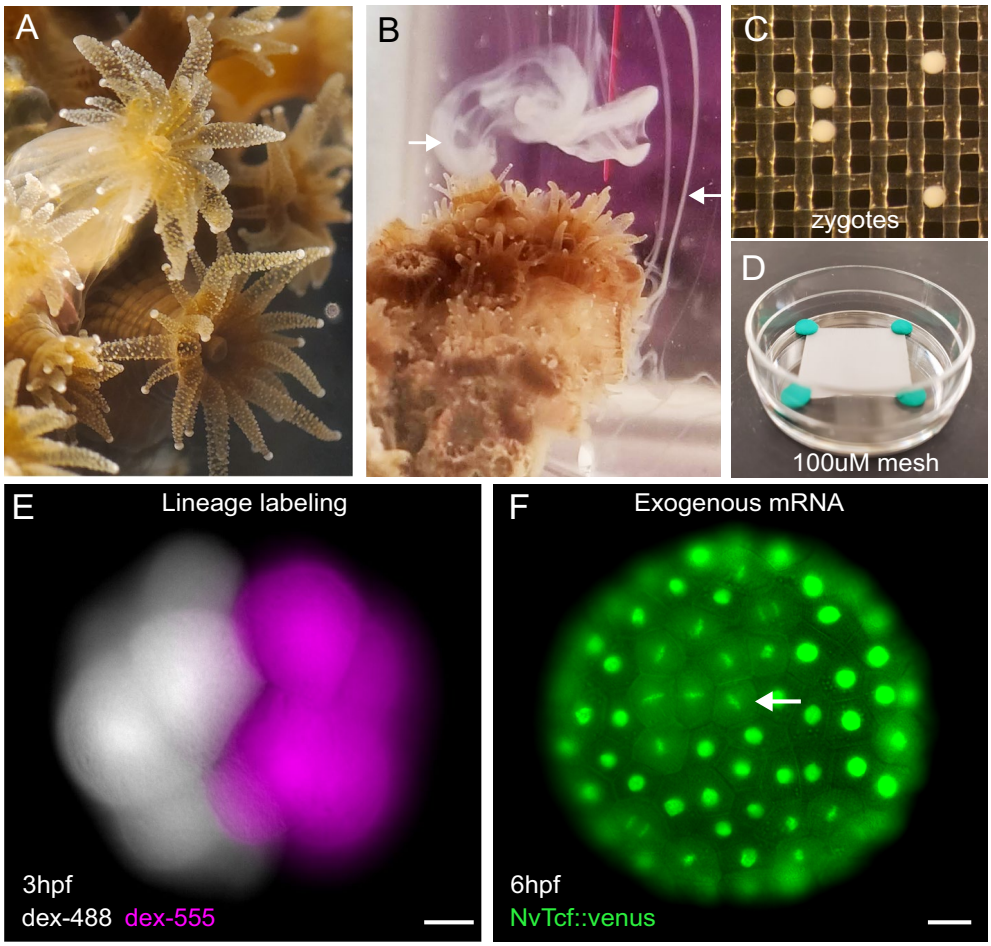

Fig. 1 *Astrangia poculata* is a tractable research organism for functional molecular studies in corals. **A** *A. poculata* colony showing extended polyps. **B** *A. poculata* colony during spawning; arrows point to sperm emerging from two polyps. **C**, **D** Zygotes resting on nylon mesh fixed in the bottom of a 35-mm petri dish in preparation for microinjection. **E** Live image of a 16-cell stage embryo injected at the 2-cell stage with two different dextran dyes (dex-488, dex-555). **F** Injection of mRNA encoding a TCF-venus fusion protein from *Nematostella vectensis* (NvTCF::venus) demonstrates proper translation and nuclear localization of exogenous mRNAs; arrow points to cells in M-phase. Scale bars = 20 µm

factor (T-cell factor/TCF) isolated from *N. vectensis*, fused to a fluorescent protein (NvTCF-venus) [49]. Blastula stage embryos exhibited nuclear localization of the fluorescent fusion protein as anticipated, and expression was maintained in healthy, dividing cells throughout early development (Fig. 1F). These results demonstrate effective expression of exogenous mRNAs, opening the possibility of using mis-expression approaches to study gene regulatory network diversification across species.

Short hairpin RNAs enable efficient gene knockdown

RNA interference techniques have become indispensable for studies of early development as they allow for efficient, robust knockdown of gene function across cell and tissue types. Among cnidarians, RNAi technologies have been successful for manipulating gene function in a wide array of taxa, including both hydrozoans [13, 14, 34, 36, 46] and anthozoans [15, 23, 63]. Recently, short hairpin RNAs (shRNA) have become a widely adopted approach for RNA interference as they can be synthesized in the lab, thereby enabling cost-effective silencing of numerous target genes [23]. We tested the efficacy of shRNA knockdown in *A. poculata* by inhibiting the activity of Fibroblast growth factor A1 (FgfA1). In *N. vectensis*, the role of FGF signaling during embryonic patterning has been well-studied [19, 37, 48, 55] and this pathway is known to be required for the formation of the apical tuft, a sensory structure at the aboral end of the larva from which a group of long cilia emerge [48]. While the apical tuft is found throughout sea anemones, most coral larvae lack this structure. The presence of an apical tuft in the larval stage of *A. poculata* [58] provides an opportunity to investigate the mechanisms driving the development and evolution of this structure across anthozoans.

Using in situ hybridization, we demonstrate that FgfA1 expression was first detected in the aboral ectoderm around the onset of gastrulation (Fig. 2A). At later stages, this expression domain becomes resolved into a focal spot on the aboral pole, consistent with the development of the apical sensory organ. To inhibit Fgf1A function in *A. poculata*, we injected zygotes with either a shRNA targeting the 3′ end of the FgfA1 transcript (see Materials and methods) or a scrambled control shRNA [25]. Animals were then raised to the larval stage at room temperature and inspected for evidence of an apical tuft. At 48 hpf, 10/10 of the knockdown larvae lacked apical tuft cilia, consistent with an inhibition of FgfA1 function (Fig. 2B). To further support a role for FgfA1 in regulating apical tuft development, we treated a separate group of zygotes with the MEK/ERK inhibitor SU5402 (20 μM), which has previously been shown to inhibit FgfA1-mediated control of apical tuft development in *N. vectensis* [48]. Treatment with SU5402 effectively phenocopied FgfA1 shRNA knockdown (Fig. 2C), resulting in the complete loss of an apical tuft in 12/12 larvae at 48hpf. These phenotypes were quantified by measuring the length of the longest cilium at the aboral end of each larva. The aboral cilia of the FgfA1 knockdown animals were significantly shorter than those in both the wild type and control shRNA-injected larvae (Fig. 2D). Likewise, we observed a significant reduction in the length of cilia at the aboral pole in SU5402-treated larvae, relative to DMSO controls (Fig. 2D). These experiments demonstrate that shRNA injection is an effective method for gene knockdown in corals and confirm that apical tuft development requires similar signaling pathways in two distantly related anthozoans (*N. vectensis* and *A. poculata*) (Fig. 2E). Pharmacological inhibition of FGF signaling has also been shown to inhibit settlement and metamorphosis in *Acropora millepora*, a species that lacks an apical tuft [9, 57]. With access to this inexpensive and effective method for gene knockdown it is now possible to interrogate the evolution of the FGF signaling pathway controlling apical sensory organ development in cnidarians with diverse larval body plans.

Development of a transgenic knock-in coral to study cnidocyte development

Genome editing approaches using CRISPR/Cas9 technology have already been used for loss-of-function analysis in a variety of cnidarians including the sea anemone *Nematostella vectensis*, the hard coral *Acropora millepora,* and the hydroids *Hydractinia symbiolongicarpus* and *Clytia hemisphaerica* [9, 18, 24, 39]. Endogenous tagging of native proteins with fluorescent markers using CRISPR-mediated homology-directed repair (HDR) has further enabled precise tagging of individual proteins and careful analysis of protein activity in vivo in *N. vectensis* and *H. symbiolongicarpus* [24, 33, 41, 50]. To date, however, successful gene knock-in in corals has not been reported. To establish a method for CRISPR-mediated gene knock-in in *A. poculata*, we tested a method that uses PCR-generated micro-homology fragments to induce HDR after CRISPR–Cas9 cleavage [53]. The benefit of this method is that knock-in repair templates can be constructed rapidly and inexpensively by PCR, without the need for cloning. To test the efficacy of CRISPR-mediated knock-in, we tagged the cnidocyte-specific marker gene, Minicollagen3 (*Mcol3*), with the fluorescent protein, mNeonGreen (mNeon). Minicollagens are found only in cnidocytes, making the expression of *Mcol3* a specific and robust marker of cnidocyte development [11]. Fluorescent labeling of cnidocytes in vivo enables future studies tracking the development and regeneration of these cells in real time.

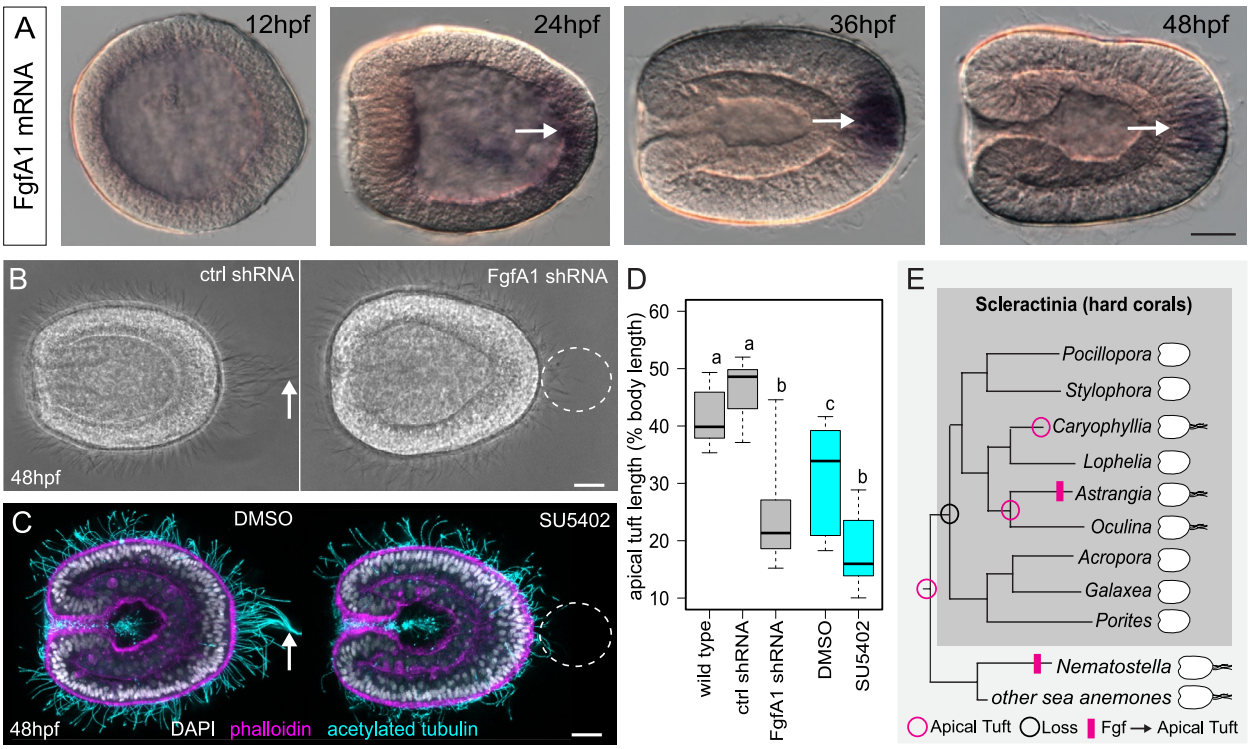

Fig. 2 Knockdown of FgfA1 induces loss of the apical tuft. **A** In situ hybridization showing the expression of FgfA1 mRNA in the aboral ectoderm of wild type embryos (*arrows*) at/after 24hpf. **B** Live images of 48 hpf larvae injected with scrambled control shRNA (ctrl shRNA) or FgfA1 shRNA. **C** Images of fixed, 48 hpf larvae treated with 20 µm SU5402 or vehicle control (DMSO) and stained with DAPI (nuclei), phalloidin (F-actin), and anti-acetylated tubulin antibody (cilia). *Arrows* in **B**, **C** point to apical tuft cilia and dotted circles indicate loss of apical tuft. The oral pole is to the left in **A**–**C**; scale bars = 20 µm. **D** Quantitative analysis of apical tuft cilia length in the shRNA experiment (*grey boxes*) and pharmacological experiment (*cyan boxes*). Box plots are presented as: median—middle line, 25th and 75th percentiles—box, 5th and 95th percentiles—whiskers. Sample sizes for each treatment: wild type N = 10, ctrl shRNA N = 8, FgfA1 shRNA N = 10, DMSO N = 10, SU5402 N = 12. P-values from ANOVA with Tukey HSD post hoc: wild type vs. ctrl shRNA: $p = 0.5839021$, wild type vs. FgfA1 shRNA: $p = 0.0000064$, ctrl shRNA vs FgfA1 shRNA: $p = 0.0000001$, wild type vs DMSO: $p = 0.0154365$, DMSO vs SU5402: $p = 0.0004114$, FgfA1 shRNA vs. SU5402: $p = 0.3147784$. *Letters* indicate groups that are significantly different. **E** Cladogram of hard corals and sea anemones plotting the distribution of taxa with a larval apical tuft (cartoons, *right*). The apical tuft was likely lost in the ancestor of Scleractinia (*black circle*) and regained in the ancestor of the clade containing *Astrangia* and *Oculina* and at least one species of Caryophyllia (*magenta circles*). An Fgf signaling pathway controls apical tuft development in *Astrangia poculata* (this study) and *Nematostella vectensis* [48]. The cladogram was inferred from two studies of overlapping taxa [27, 38]. References indicating presence/absence of apical tuft by taxon: *Pocillopora* [60], *Stylophora* [1], *Caryophyllia* [61], *Lophelia* [30], *Astrangia* [58], *Oculina* [5], *Acropora* [22], *Galaxea* [1], *Porites* [51], *Nematostella* [21], other sea anemones: *Anthopleura* [7], *Exaiptasia* [6], *Gonactinia* [8]

We designed two single guide RNAs (sgRNAs) targeting the stop codon of the last exon of *Mcol3* and used an HDR repair template to insert the sequence of mNeon downstream of and in frame with *Mcol3* (Fig. 3A). After injecting this repair template along with the sgRNAs and Cas9 protein, we observed positive fluorescent signal in developing cnidocytes beginning at 36hpf in approximately 10% (11/120) of injected larvae (Fig. 3B). Knock-in larvae exhibited mosaic expression of Mcol3::mNeon, a common outcome of CRISPR-mediated genome editing likely representing a repair event that occurred at later embryonic stages. We confirmed positive integration using PCR with primers that flank mNeon to discriminate wild type alleles from mutant alleles with gel electrophoresis (Fig. 3C). Using in situ hybridization, we confirmed that the knock-in construct recapitulated endogenous expression, showing that *Mcol3* is expressed in a salt and pepper pattern in the ectoderm during embryogenesis in *A. poculata* (Fig. 3D), a pattern consistent with the development of cnidocytes in *N. vectensis* [64]. Mature cnidocytes are visible in the larva at 48 hpf, shortly after the onset of expression of *Mcol3* (Fig. 3E). Together, these data show that the timing and distribution of fluorescent cells observed in knock-in larvae are consistent with the endogenous expression of *Mcol3* mRNA in *A. poculata* and the appearance of mature cnidocytes in wild type larvae. Cnidocytes are thought to have evolved from a neural-like precursor in the ancestor

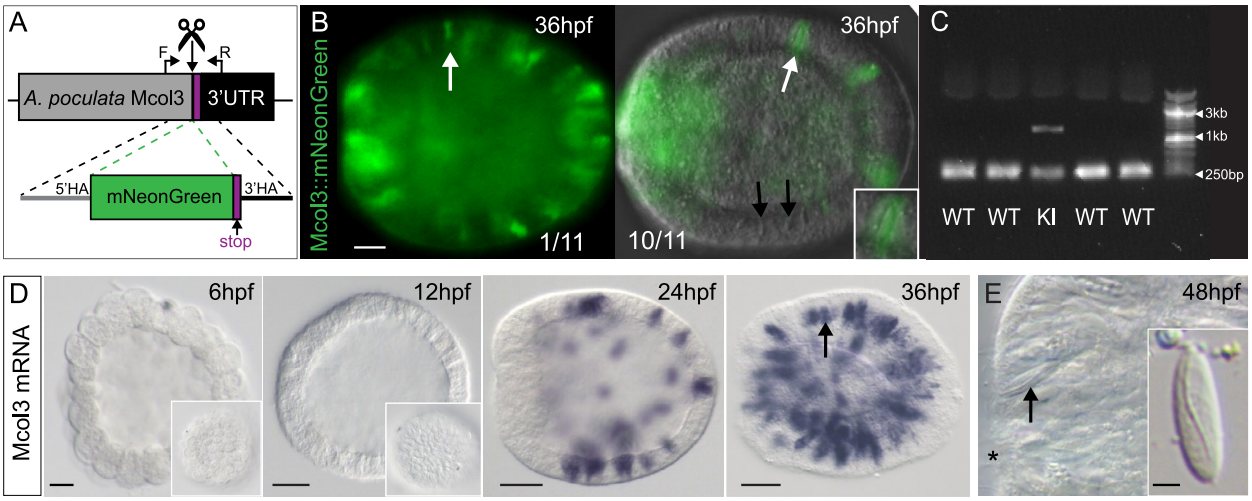

Fig. 3 Endogenous labeling of developing cnidocytes using CRISPR/Cas9 genome editing. **A** Schematic showing knock-in strategy with relative position of sgRNA (scissors), genotyping primers (F/R, *bent arrows*), and repair template, including left and right homology arms (5'HA, 3'HA). The stop codon is indicated in purple. **B** Live images of embryos either weakly mosaic (1/11 embryos) or strongly mosaic (10/11 embryos) fluorescent expression of *Mcol3*::mNeon; labeled cnidocytes (*white arrows*) are distributed throughout the ectoderm. *Black arrows* show unlabeled cnidocytes. **C** Agarose gel genotyping of five individual embryos, one knock-in mutant (KI—same embryo pictured in **B**, *left*) and four wild types (WT). The wild type amplicon (350 bp) is present in all five embryos and the amplicon containing the mNeon insert (1060 bp) is present only in the mutant. **D** In situ hybridization confirms the timing and distribution of cells expressing *Mcol3* mRNA (immature cnidocytes) in the ectoderm at/after 24 hpf. *Insets* show surface detail and *arrow points* to *Mcol3*-expressing immature cnidocytes. **E** Mature cnidocytes are detected in the ectoderm at 48 hpf. DIC image of the oral region of a 48 hpf larva. *Inset* shows an isolated cnidocyte extracted from a dissociated larva; arrow points to a mature cnidocyte in situ. The oral pole is to the left in **B**, **D**, **E**; the position of the blastopore is marked by * in **E**. Scale bars in **B**, **D** = 20 µm; scale bar in **E** = 2 µm

of cnidarians [2], yet our understanding of the complex regulatory interactions that drive diversification of cnidocyte form and function remains limited [3]. The ability to track early cnidocyte development in vivo using endogenously tagged proteins in *A. poculata* makes this animal a critical model for understanding diversification of this phylum-restricted cell type.

Conclusions

Due to the ease of collection and the ability to control the timing of spawns in the lab, *Astrangia poculata* is a tractable organism for functional genomic studies in hard corals. Their hardy, transparent embryos are robust to microinjection and genetic manipulation. We show that gene silencing and overexpression can be achieved by microinjection using low-cost techniques. We also show that exogenous gene knock-in can be readily achieved using a repair template generated by PCR to induce HDR following a CRISPR/Cas9 cutting reaction. *Astrangia poculata* has been recognized as a valuable experimental system for investigative studies of coral–microbe interactions [43], and the tools presented here make this animal a viable system for comparative studies of cnidarian evolution and development (Fig. 4). One current challenge with this system is that it is not yet possible to complete the lifecycle of *A. poculata* in the laboratory. Future

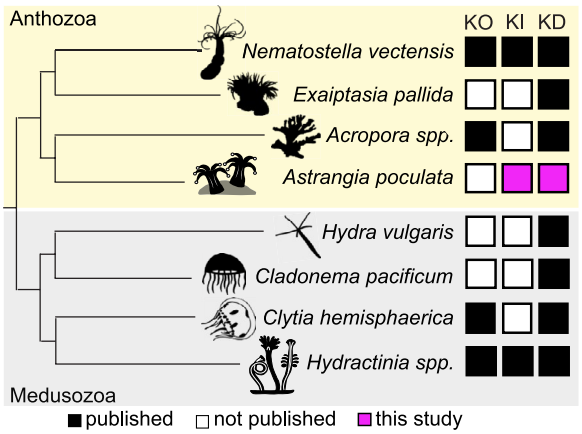

Fig. 4 Summary of functional genomic tools available in cnidarians. KO—knockout, KI—knock-in, KD—knockdown by RNA interference. References by taxon: *Nematostella vectensis* [23, 24, 41], *Exaiptasia pallida* [15], *Acropora millepora* (KO) [9], *Acropora tenuis* (KD) [63], *Astrangia poculata* (this study), *Hydra vulgaris* [34], *Cladonema pacificum* [36], *Clytia hemisphaerica* (KO) [39, 45], *Clytia hemisphaerica* (KD) [36], *Hydractinia echinata* (KO, KD) [14, 18], *Hydractinia symbiolongicarpus* (KI, KD) [13, 46, 50]. The cladogram was inferred from two studies of overlapping taxa [16, 26]. Silhouettes were downloaded from Phylopic.org, license (CC BY-SA 3.0)

studies aimed at identifying the cues necessary to induce larval settlement are a critical next step in developing this animal for studies of adult characteristics including symbiosis and calcification. We anticipate that the functional genomic techniques described here can be readily adapted for studying early development in other coral species and will accelerate research on fundamental cellular and molecular processes in corals and enable finer scale comparisons of comparative development in Anthozoa.

Author contributions
JFW, RB, AS, EB, IVC, KS and LSB collected data and performed analyses; JFW and LSB conceived of the study and wrote the manuscript; RB, AS, EB, IVC, and KS edited and approved the manuscript.

Funding
This work was supported by the North Carolina Biotechnology Center (2022-FLG-3803, J.F.W.) and the National Institutes of Health (R15GM139113-01A1 to J.F.W., R35GM147253-01 to L.S.B., and P20GM103430 to K.S.)

Availability of data and materials
The transcriptome assembly used for cloning, primer design, and knock-in construct design has been deposited at the NCBI repository (PRJNA956119) and is publicly available as of the date of publication. All transcript, primer, and donor sequences associated with this manuscript are provided in the Methods.

Declarations

Competing interests
The authors declare no competing interests.

Received: 19 March 2025 Accepted: 2 May 2025
Published online: 16 May 2025

References

1. Atoda K. The larva and postlarval development of the reef-building corals IV. Galaxea aspera quelch. J Morphol. 1951;89:17–35.
2. Babonis LS, Enjolras C, Ryan JF, Martindale MQ. A novel regulatory gene promotes novel cell fate by suppressing ancestral fate in the sea anemone *Nematostella vectensis*. Proc Natl Acad Sci. 2022;119: e2113701119.
3. Babonis LS, Enjolras C, Reft AJ, Foster BM, Hugosson F, Ryan JF, Daly M, Martindale MQ. Single-cell atavism reveals an ancient mechanism of cell type diversification in a sea anemone. Nat Commun. 2023;14:885.
4. Bolger AM, Lohse M, Usadel B. Trimmomatic: a flexible trimmer for Illumina sequence data. Bioinformatics. 2014;30:2114–20.
5. Brooke S, Young C. Reproductive ecology of a deep-water scleractinian coral, *Oculina varicosa*, from the southeast Florida shelf. Cont Shelf Res. 2003;23:847–58.
6. Bucher M, Wolfowicz I, Voss PA, Hambleton EA, Guse A. Development and symbiosis establishment in the cnidarian endosymbiosis model *Aiptasia* sp. Sci Rep. 2016;6:19867.
7. Chia F-S, Koss R. Fine structural studies of the nervous system and the apical organ in the planula larva of the sea anemone *Anthopleura elegantissima*. J Morphol. 1979;160:275–97.
8. Chia F-S, Lützen J, Svane I. Sexual reproduction and larval morphology of the primitive anthozoan *Gonactinia prolifera* M. Sars. J Exp Mar Biol Ecol. 1989;127:13–24.
9. Cleves PA, Strader ME, Bay LK, Pringle JR, Matz MV. CRISPR/Cas9-mediated genome editing in a reef-building coral. Proc Natl Acad Sci. 2018;115:5235–40.
10. Crawford K, Diaz Quiroz JF, Koenig KM, Ahuja N, Albertin CB, Rosenthal JJC. Highly efficient knockout of a squid pigmentation gene. Curr Biol CB. 2020;30:3484-3490.e4.
11. David CN, Özbek S, Adamczyk P, Meier S, Pauly B, Chapman J, Hwang JS, Gojobori T, Holstein TW. Evolution of complex structures: minicollagens shape the cnidarian nematocyst. Trends Genet. 2008;24:431–8.
12. Dimond J, Kerwin A, Rotjan R, Sharp K, Stewart F, Thornhill D. A simple temperature-based model predicts the upper latitudinal limit of the temperate coral *Astrangia poculata*. Coral Reefs. 2013;32:401–9.
13. DuBuc TQ, Schnitzler CE, Chrysostomou E, McMahon ET, Febrimarsa, Gahan JM, Buggie T, Gornik SG, HanleyBarreira SSN, et al. Transcription factor AP2 controls cnidarian germ cell induction. Science. 2020;367:757–62.
14. Duffy DJ, Plickert G, Kuenzel T, Tilmann W, Frank U. Wnt signaling promotes oral but suppresses aboral structures in Hydractinia metamorphosis and regeneration. Development. 2010;137:3057–66.
15. Dunn SR, Phillips WS, Green DR, Weis VM. Knockdown of actin and caspase gene expression by RNA interference in the symbiotic anemone *Aiptasia pallida*. Biol Bull. 2007;212:250–8.
16. Fang X, Zhou K, Chen J. The complete linear mitochondrial genome of the hydrozoan jellyfish *Cladonema multiramosum* Zhou et al., 2022 (Cnidaria: Hydrozoa: Cladonematidae). Mitochondrial DNA Part B Resour. 2022;7:921–3.
17. Fritzenwanker JH, Genikhovich G, Kraus Y, Technau U. Early development and axis specification in the sea anemone *Nematostella vectensis*. Dev Biol. 2007;310:264–79.
18. Gahan JM, Schnitzler CE, DuBuc TQ, Doonan LB, Kanska J, Gornik SG, Barreira S, Thompson K, Schiffer P, Baxevanis AD, et al. Functional studies on the role of Notch signaling in Hydractinia development. Dev Biol. 2017;428:224–31.
19. Gilbert E, Teeling C, Lebedeva T, Pedersen S, Chrismas N, Genikhovich G, Modepalli V. Molecular and cellular architecture of the larval sensory organ in the cnidarian *Nematostella vectensis*. Dev Camb Engl. 2022;149:dev200833.
20. Grabherr MG, Haas BJ, Yassour M, Levin JZ, Thompson DA, Amit I, Adiconis X, Fan L, Raychowdhury R, Zeng Q, et al. Full-length transcriptome assembly from RNA-Seq data without a reference genome. Nat Biotechnol. 2011;29:644–52.
21. Hand C, Uhlinger KR. The culture, sexual and asexual reproduction, and growth of the sea anemone *Nematostella vectensis*. Biol Bull. 1992;182:169–76.
22. Hayward DC, Grasso LC, Saint R, Miller DJ, Ball EE. The organizer in evolution–gastrulation and organizer gene expression highlight the importance of Brachyury during development of the coral, *Acropora millepora*. Dev Biol. 2015;399:337–47.
23. He S, del Viso F, Chen C-Y, Ikmi A, Kroesen AE, Gibson MC. An axial Hox code controls tissue segmentation and body patterning in *Nematostella vectensis*. Science. 2018;361:1377–80.
24. Ikmi A, McKinney SA, Delventhal KM, Gibson MC. TALEN and CRISPR/Cas9-mediated genome editing in the early-branching metazoan *Nematostella vectensis*. Nat Commun. 2014;5:5486.
25. Karabulut A, He S, Chen C-Y, McKinney SA, Gibson MC. Electroporation of short hairpin RNAs for rapid and efficient gene knockdown in the starlet sea anemone, *Nematostella vectensis*. Dev Biol. 2019;448:7–15.
26. Kayal E, Bentlage B, Sabrina Pankey M, Ohdera AH, Medina M, Plachetzki DC, Collins AG, Ryan JF. Phylogenomics provides a robust topology of the major cnidarian lineages and insights on the origins of key organismal traits. BMC Evol Biol. 2018;18:68.
27. Kitahara MV, Cairns SD, Stolarski J, Blair D, Miller DJ. A Comprehensive phylogenetic analysis of the Scleractinia (Cnidaria, Anthozoa) based on mitochondrial CO1 sequence data. PLoS ONE. 2010;5: e11490.
28. Labun K, Montague TG, Krause M, Torres Cleuren YN, Tjeldnes H, Valen E. CHOPCHOP v3: expanding the CRISPR web toolbox beyond genome editing. Nucleic Acids Res. 2019;47:W171–4.
29. Langmead B, Salzberg SL. Fast gapped-read alignment with Bowtie 2. Nat Methods. 2012;9:357–9.
30. Larsson AI, Järnegren J, Strömberg SM, Dahl MP, Lundälv T, Brooke S. Embryogenesis and larval biology of the cold-water coral *Lophelia pertusa*. PLoS ONE. 2014;9: e102222.

31. Layden MJ, Röttinger E, Wolenski FS, Gilmore TD, Martindale MQ. Microinjection of mRNA or morpholinos for reverse genetic analysis in the starlet sea anemone, *Nematostella vectensis*. Nat Protoc. 2013;8:924–34.
32. Layden MJ, Rentzsch F, Röttinger E. The rise of the starlet sea anemone *Nematostella vectensis* as a model system to investigate development and regeneration: Overview of starlet sea anemone *Nematostella vectensis*. Wiley Interdiscip Rev Dev Biol. 2016;5:408–28.
33. Lebedeva T, Boström J, Kremnyov S, Mörsdorf D, Niedermoser I, Genikhovich E, Hejnol A, Adameyko I, Genikhovich G. β-catenin-driven endomesoderm specification is a Bilateria-specific novelty. Nat Commun. 2025;16:2476.
34. Lohmann JU, Endl I, Bosch TC. Silencing of developmental genes in Hydra. Dev Biol. 1999;214:211–4.
35. Martin M. Cutadapt removes adapter sequences from high-throughput sequencing reads. EMBnet J. 2011;17:10.
36. Masuda-Ozawa T, Fujita S, Nakamura R, Watanabe H, Kuranaga E, Nakajima Y. siRNA-mediated gene knockdown via electroporation in hydrozoan jellyfish embryos. Sci Rep. 2022;12:16049.
37. Matus DQ, Thomsen GH, Martindale MQ. FGF signaling in gastrulation and neural development in *Nematostella vectensis*, an anthozoan cnidarian. Dev Genes Evol. 2007;217:137–48.
38. McFadden CS, Quattrini AM, Brugler MR, Cowman PF, Dueñas LF, Kitahara MV, Paz-García DA, Reimer JD, Rodríguez E. Phylogenomics, origin, and diversification of anthozoans (Phylum Cnidaria). Syst Biol. 2021;70:635–47.
39. Momose T, De Cian A, Shiba K, Inaba K, Giovannangeli C, Concordet J-P. High doses of CRISPR/Cas9 ribonucleoprotein efficiently induce gene knockout with low mosaicism in the hydrozoan *Clytia hemisphaerica* through microhomology-mediated deletion. Sci Rep. 2018;8:11734.
40. Oulhen N, Pieplow C, Perillo M, Gregory P, Wessel GM. Optimizing CRISPR/Cas9-based gene manipulation in echinoderms. Dev Biol. 2022;490:117–24.
41. Paix A, Basu S, Steenbergen P, Singh R, Prevedel R, Ikmi A. Endogenous tagging of multiple cellular components in the sea anemone *Nematostella vectensis*. Proc Natl Acad Sci. 2023;120: e2215958120.
42. Presnell JS, Browne WE. Krüppel-like factor gene function in the ctenophore Mnemiopsis leidyi assessed by CRISPR/Cas9-mediated genome editing. Dev Camb Engl. 2021;148:199771.
43. Puntin G, Sweet M, Fraune S, Medina M, Sharp K, Weis VM, Ziegler M. Harnessing the power of model organisms to unravel microbial functions in the coral holobiont. Microbiol Mol Biol Rev MMBR. 2022;86: e0005322.
44. Quast C, Pruesse E, Yilmaz P, Gerken J, Schweer T, Yarza P, Peplies J, Glöckner FO. The SILVA ribosomal RNA gene database project: improved data processing and web-based tools. Nucleic Acids Res. 2013;41:D590–6.
45. Quiroga Artigas G, Lapébie P, Leclère L, Takeda N, Deguchi R, Jékely G, Momose T, Houliston E. A gonad-expressed opsin mediates light-induced spawning in the jellyfish Clytia. Elife. 2018;7:e29555.
46. Quiroga-Artigas G, Duscher A, Lundquist K, Waletich J, Schnitzler CE. Gene knockdown via electroporation of short hairpin RNAs in embryos of the marine hydroid *Hydractinia symbiolongicarpus*. Sci Rep. 2020;10:12806.
47. R Core Team. 2020. R: A language and environment for statistical computing. R Found. Stat. Comput. Vienna Austria.
48. Rentzsch F, Fritzenwanker JH, Scholz CB, Technau U. FGF signalling controls formation of the apical sensory organ in the cnidarian *Nematostella vectensis*. Development. 2008;135:1761–9.
49. Röttinger E, Dahlin P, Martindale MQ. A framework for the establishment of a cnidarian gene regulatory network for "endomesoderm" specification: The inputs of ß-Catenin/TCF signaling. PLoS Genet. 2012;8: e1003164.
50. Sanders SM, Ma Z, Hughes JM, Riscoe BM, Gibson GA, Watson AM, Flici H, Frank U, Schnitzler CE, Baxevanis AD, et al. CRISPR/Cas9-mediated gene knockin in the hydroid *Hydractinia symbiolongicarpus*. BMC Genomics. 2018;19:649.
51. Santiago-Valentín J-D, Rodríguez-Troncoso A-P, Bautista-Guerrero E, López-Pérez A, Cupul-Magaña A-L, Santiago-Valentín J-D, Rodríguez-Troncoso A-P, Bautista-Guerrero E, López-Pérez A, Cupul-Magaña A-L. Internal ultrastructure of the planktonic larva of the coral *Porites panamensis* (Anthozoa: Scleractinia). Rev Biol Trop. 2022;70:222–34.
52. Schindelin J, Arganda-Carreras I, Frise E, Kaynig V, Longair M, Pietzsch T, Preibisch S, Rueden C, Saalfeld S, Schmid B, et al. Fiji: an open-source platform for biological-image analysis. Nat Methods. 2012;9:676–82.
53. Seleit A, Aulehla A, Paix A. Endogenous protein tagging in medaka using a simplified CRISPR/Cas9 knock-in approach. Elife. 2021;10:e75050.
54. Servetnick MD, Steinworth B, Babonis LS, Simmons D, Salinas-Saavedra M, Martindale MQ. Cas9-mediated excision of *Nematostella brachyury* disrupts endoderm development, pharynx formation, and oral–aboral patterning. Development. 2017;144:2951–60.
55. Sinigaglia C, Busengdal H, Lerner A, Oliveri P, Rentzsch F. Molecular characterization of the apical organ of the anthozoan *Nematostella vectensis*. Dev Biol. 2015;398:120–33.
56. Song L, Florea L. Rcorrector: efficient and accurate error correction for Illumina RNA-seq reads. GigaScience. 2015;4:48.
57. Strader ME, Aglyamova GV, Matz MV. Molecular characterization of larval development from fertilization to metamorphosis in a reef-building coral. BMC Genomics. 2018;19:17.
58. Szmant-Froelich A, Yevich P, Pilson MEQ. Gametogenesis and early development of the temperate coral *Astrangia danae* (Anthozoa: Scleractinia). Biol Bull. 1980;158:257–69.
59. Tinoco AI, Mitchison-Field LMY, Bradford J, Renicke C, Perrin D, Bay LK, Pringle JR, Cleves PA. Role of the bicarbonate transporter SLC4γ in stony-coral skeleton formation and evolution. Proc Natl Acad Sci. 2023;120: e2216144120.
60. Tran C, Hadfield MG. Localization of sensory mechanisms utilized by coral planulae to detect settlement cues. Invertebr Biol. 2013;132:195–206.
61. Tranter PRG, Nicholson DN, Kinchington D. A description of spawning and post-gastrula development of the cool temperate coral, Caryophyllia Smithi. J Mar Biol Assoc U K. 1982;62:845–54.
62. Wolenski FS, Layden MJ, Martindale MQ, Gilmore TD, Finnerty JR. Characterizing the spatiotemporal expression of RNAs and proteins in the starlet sea anemone, *Nematostella vectensis*. Nat Protoc. 2013;8:900–15.
63. Yuyama I, Higuchi T, Hidaka M. Application of RNA interference technology to acroporid juvenile corals. Front Mar Sci. 2021;2:1–9. https://doi.org/10.3389/fmars.2021.688876.
64. Zenkert C, Takahashi T, Diesner M-O, Özbek S. Morphological and molecular analysis of the *Nematostella vectensis* cnidom. PLoS ONE. 2011;6: e22725.

Publisher's Note